Two-Dimensional and Full Polarimetric Imaging by a Synthetic Aperture FM-CW Radar

Yoshio Yamaguchi, *Senior Member, IEEE*, Toru Nishikawa, Masakazu Sengoku, *Senior Member, IEEE*, and Wolfgang-Martin Boerner, *Fellow, IEEE*

***Abstract*—This paper applies the principle of radar polarimetry to a synthetic aperture frequency-modulated continuous wave (FM-CW) radar and presents results based on two-dimensional (2-D) full polarimetric imaging. It is shown that the polarimetric target reflection coefficients obtained by the synthetic aperture FM-CW radar are elements of a Sinclair scattering matrix, although the coefficients are derived from a wide band signal. Using the scattering matrix optimization procedure, a 2-D polarimetric imaging experiment (including Co-Pol maximum, minimum, span, and phase imaging) of an orthogonally placed linear target set was successfully carried out in the laboratory. This result demonstrates the validity of X-band (8.2–9.2 GHz) FM-CW radar polarimetry, and it presents a demonstration of a full polarimetric 2-D FM-CW imaging radar system.**

I. Introduction

RADAR polarimetry, i.e., the full utilization of the vector nature of electromagnetic wave information, has become an indispensable tool for advanced high resolution radar sensing systems [1], [2]. If the principle of radar polarimetry [1]–[6] could be incorporated into the wide band FM-CW radar, it would become a highly advanced high resolution imaging system in the short range sensing, since the FM-CW radar utilizes the continuous wave principle for which the range resolution is determined by the frequency resolution. In addition, it displays the potential ability for precisely measuring distances in the near range with considerably simpler instrumentation as compared to pulsed radar systems [7], [8]. Our research goal is to develop a full polarimetric and synthetic aperture FM-CW imaging radar aimed at detecting and mapping objects in free space, or in snowpack and/or occluded underground [9], [10]. However, the principle of wide band FM-CW polarimetry is still in the development phase, although the principle for the monochromatic (single frequency) wave has already been well established [1], [2].

This paper extends the earlier work [11] (on the one-dimensional case) and incorporates the principle of radar polarimetry into a 2-D synthetic aperture FM-CW radar system, and presents a full polarimetric imaging result of linear targets. The main purpose of this paper is to show experimentally that the FM-CW radar acts as a full polarimetric and 2-D imaging radar system if we regard the polarimetric target reflection coefficients obtained by a synthetic aperture processing as the elements of Sinclair scattering matrix, provided that the scattering characteristics are almost constant within the operational bandwidth. For this purpose, we carried out a 2-D imaging experiment to confirm the theory.

In the following, the principles of polarimetric imaging for the monochromatic wave case are briefly introduced in Section II. The principle of 2-D synthetic aperture FM-CW radar is outlined in Section III showing that a target reflection coefficient may be replaced by a scattering matrix element. Section IV is devoted to confirm the validity by showing an experimental 2-D polarimetric image of orthogonally placed metallic pipes, including the Co-Pol maximum and span images. Also, an attempt was made to pick up target images by a scattering matrix phase term when the magnitude of the reflected signal is small. It is shown and concluded that radar polarimetry can be applied to the 2-D FM-CW radar imaging.

II. Polarimetric Imaging Using the Scattering Matrix Optimization Procedure

In this section, a brief introduction of polarimetric imaging using scattering matrix optimization procedures [5], [6] is given. If a Sinclair scattering matrix $[S]$ is measured in the polarization basis *(HV)*.

$$[S(HV)] = \begin{bmatrix} S_{HH} & S_{HV} \\ S_{VH} & S_{VV} \end{bmatrix} \tag{1}$$

it is possible to compute the Co-Pol channel power P_c according to

$$P_c = \left|\mathbf{E}_t(HV)^T [S(HV)] \mathbf{E}_t(HV)\right|^2 \tag{2}$$

where $\mathbf{E}_t(HV)$ represents the polarization state of a radar transmitter and T denotes transpose. The Co-Pol channel means that the receiving antenna has a polarization state identical with the transmitter. In the above expression, the amplitude factor due to path length and transducer antenna properties are omitted because we are interested in primarily in polarimetric information [3]. The $\mathbf{E}_t(HV)$ is defined by Jones vector form

$$\mathbf{E}_t(HV) = \frac{1}{\sqrt{1+\rho\rho^*}} \begin{bmatrix} 1 \\ \rho \end{bmatrix} \tag{3}$$

where ρ is the polarization ratio. The polarization ratio is defined by the ratio of two orthogonal components of $\mathbf{E}_t$ in

Manuscript received December 16, 1993. This work was supported in part by a Grant-in-Aid for Scientific Research of the Ministry of Education, Japan.

Y. Yamaguchi, T. Nishikawa, and M. Sengoku are with the Department of Information Engineering, Faculty of Engineering, Niigata University, Niigata-shi 950-21, Japan.

W. M. Boerner is with the Department of Electrical Engineering and Computer Science, University of Illinois, Chicago, IL 60607–7018 USA.

IEEE Log Number 9407850.

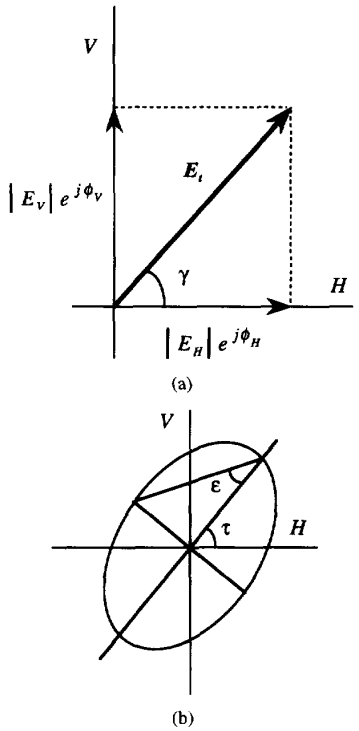

Fig. 1. Polarization state. (a) in the HV basis, (b) polarization ellipse in terms of geometric parameters ε and τ.

the basis (HV) as

$$\rho = \frac{E_V}{E_H} = \left|\frac{E_V}{E_H}\right| e^{j(\phi_V - \phi_H)} = |\rho| e^{j\delta} = \tan\gamma e^{j\delta}. \quad (4)$$

The parameters of γ and $\delta = \phi_V - \phi_H$ are related to the geometric parameters of the polarization ellipse (see Fig. 1) as

$$\tan 2\tau = \tan 2\gamma \cos\delta, \quad (5a)$$

$$\sin 2\varepsilon = \sin 2\gamma \sin\delta, \quad (5b)$$

where ε and τ are ellipticity angle ($-\pi/4 \leq \varepsilon \leq \pi/4$) and tilt angle ($-\pi/2 \leq \tau \leq \pi/2$), respectively.

The optimization of (2) as a function of ρ is well described in [5], [6]. The characteristic polarization state theory [6] shows that the maximum power is obtained by choosing the polarization ratio as

$$\rho_{1,2} = \frac{-B \pm \sqrt{B^2 - 4AC}}{2A}, \quad (6)$$

where

$$A = S_{HH}^* S_{HV} + S_{HV}^* S_{VV}, \quad B = |S_{HH}|^2 - |S_{VV}|^2, \quad C = -A^*.$$

The polarization states in the form of (3) using ρ_1 and ρ_2 are called Co-Pol maximum and Co-Pol extremum (saddle). Since the two polarization states are orthogonal, i.e., $\rho_1 \rho_2^* = -1$, one can constitute a new polarization basis (AB) based on ρ_1 and ρ_2. The change of polarization basis from the old basis (HV) to the new basis (AB) guarantees the invariance of the span of scattering matrix,

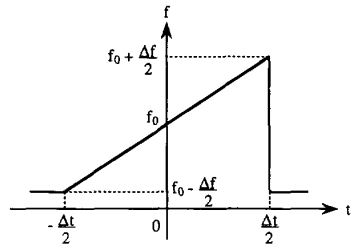

Fig. 2. Relation of frequency and time in FM-CW radars.

$$\begin{aligned}\text{Span}\{[S(AB)]\} &= |S_{AA}|^2 + |S_{AB}|^2 + |S_{BA}|^2 + |S_{BB}|^2 \\ &= |S_{HH}|^2 + |S_{HV}|^2 + |S_{VH}|^2 + |S_{VV}|^2 \\ &= \text{Span}\{[S(HV)]\}, \end{aligned} \quad (7)$$

and the invariance of power,

$$\begin{aligned} P_c &= \left|\mathbf{E}_t(HV)^T [S(HV)] \mathbf{E}_t(HV)\right|^2 \\ &= \left|\mathbf{E}_t(AB)^T [S(AB)] \mathbf{E}_t(AB)\right|^2. \end{aligned} \quad (8)$$

A similar theory applies to the Co-Pol minimum polarization states which give $P_c = 0$. Also the theory applies to the Cross (X)-Pol channel case, where the polarization state of the receiver antenna is orthogonal to the transmitter polarization.

The above discussion implies that polarimetric imaging on a pixel by pixel basis can be achieved using the polarization ratio in order to enhance or eliminate a target. This is, if a target scattering matrix belonging to a pixel in a 2-D radar scene is extracted, it is possible to calculate a specific polarization ratio for which the radar channel receives optimal power, i.e., either maximum or minimum power correspondingly. Then, using the polarization ratio and the resultant polarization state, we can calculate the power in the other pixels according to (2) or (8). Hence it is possible to obtain a 2-D scene by the determined optimal polarization ratio. This methodology describes the principle of polarimetric contrast enhancement on a pixel by pixel basis.

III. Principle of 2-Dimensional Synthetic Aperture FM-CW Radar

Since the principle of FM-CW radar is well established and documented [7]–[11], only a description of the beat spectrum necessary for 2-D imaging is given. The FM-CW radar measures a target range by the beat frequency of a transmitted radar signal and received signal from the target. The transmitted signal is linearly swept from $f_0 - \frac{\Delta f}{2}$ to $f_0 + \frac{\Delta f}{2}$ with f_0 denoting the center frequency, and it is a frequency modulated wave as shown in Fig. 2. If a point target is located in the Fresnel region, shown in Fig. 3, where the antenna is scanned in the x-y plane at $z = 0$, the beat spectrum due to the target can be written as

$$U(x, y, z) = Bf(z - z_0) g(x_0, y_0, z_0) h(x - x_0, y - y_0, z_0) \quad (9)$$

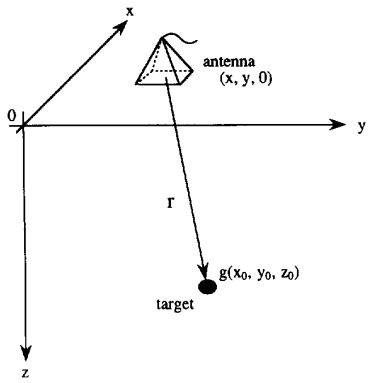

Fig. 3. Positions of antenna and point target.

where B is an amplitude, $g(x_0, y_0, z_0)$ is a point target reflection coefficient at the position of (x_0, y_0, z_0), and $f(z - z_0)$ and $h(x - x_0, y - y_0, z_0)$ are, respectively, sinc and propagation transfer functions given by

$$f(z - z_0) = \frac{\sin[\alpha(z - z_0)]}{\alpha(z - z_0)}, \quad \alpha = \frac{2\pi\Delta f}{c}, \tag{10}$$

$$h(x - x_0, y - y_0, z_0) = \exp\left[j\frac{4\pi f_0}{c}\left\{z_0 + \frac{(x - x_0)^2 + (y - y_0)^2}{2z_0}\right\}\right]. \tag{11}$$

If the target possesses a two-dimensional distribution $g = g(x_0, y_0, z_0)$ in the $z = z_0$ imaging plane, the beat spectrum received at the antenna position $(x, y, 0)$ can be written as

$$U(x, y, z) = B\int_{-\infty}^{\infty}\int_{-\infty}^{\infty} f(z - z_0)g(x_0, y_0, z_0) \times h(x - x_0, y - y_0, z_0) \times dx_0\, dy_0 \tag{12}$$

which becomes a maximum at $z = z_0$, resulting in

$$U(x, y, z_0) = B\int_{-\infty}^{\infty}\int_{-\infty}^{\infty} g(x_0, y_0, z_0) \times h(x - x_0, y - y_0, z_0) \times dx_0\, dy_0. \tag{13}$$

It is assumed here that the antenna has a wide beam so that the target can be illuminated at any antenna position $(x, y, 0)$. Because of the convolution integral form of (13), $U(x, y, z_0)$ can be regarded to be of the Fresnel hologram. The object function can therefore be obtained by an inverse convolution integral after multiplying the complex conjugated propagation transfer function h^* by U so that

$$g(x_0, y_0, z_0) = \int_{-\frac{L_x}{2}}^{\frac{L_x}{2}}\int_{-\frac{L_y}{2}}^{\frac{L_y}{2}} U(x, y, z_0)h^*(x_0 - x, y_0 - y, z_0)dx\, dy. \tag{14}$$

L_x and L_y are the antenna-scan widths in the x- and y-directions, respectively. The symbol * denotes complex conjugation. This equation establishes the basis of the 2-D synthetic aperture FM-CW radar principle. The target reflection coefficient is recovered by scanning the radar antenna in the $(x$-$y)$ plane, and the signal processing can be carried out by performing

$$g(x_0, y_0, z_0) = \mathbf{FT}^{-1}[\mathbf{FT}(U) \cdot \mathbf{FT}(h^*)] \tag{15}$$

where $\mathbf{FT}$ denotes Fourier transformation and $\mathbf{FT}^{-1}$ denotes Inverse Fourier transformation.

The above equation holds for any polarization measurement. If we measure $g(x_0, y_0, z_0)$ in the conventional (HV) basis, it is possible to obtain complete polarimetric information. In this paper, we denote the polarimetric $g(x_0, y_0, z_0)$ as g_{HV} where the first letter "H" stands for reception, and the second letter "V" for transmission. Since the value of g contains amplitude and polarimetric phase (complex quantity), we can consider correspondingly, each polarimetric g as the scattering matrix element so that

$$[S(HV)] = \begin{bmatrix} S_{HH} & S_{HV} \\ S_{VH} & S_{VV} \end{bmatrix} = \begin{bmatrix} g_{HH} & g_{HV} \\ g_{VH} & g_{VV} \end{bmatrix}. \tag{16}$$

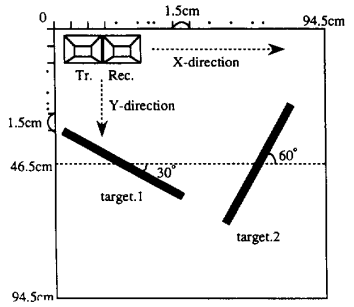

Fig. 4. Measurement scheme viewed from antenna.

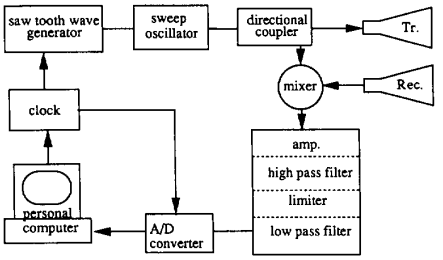

Fig. 5. Block diagram of FM-CW radar.

TABLE I
RADAR SPECIFICATION

RF power	18 dBm
Polarization	linear H,V
Polarization purity	30 dB (nominal)
Sensitivity	- 42 dBm
Sweep frequency range	8.2 - 9.2 GHz
Sweep time	5.2 msec
Range accuracy	1.52 cm
Scanning area	94.5 x 94.5 cm^2
Scanning interval	1.5 cm

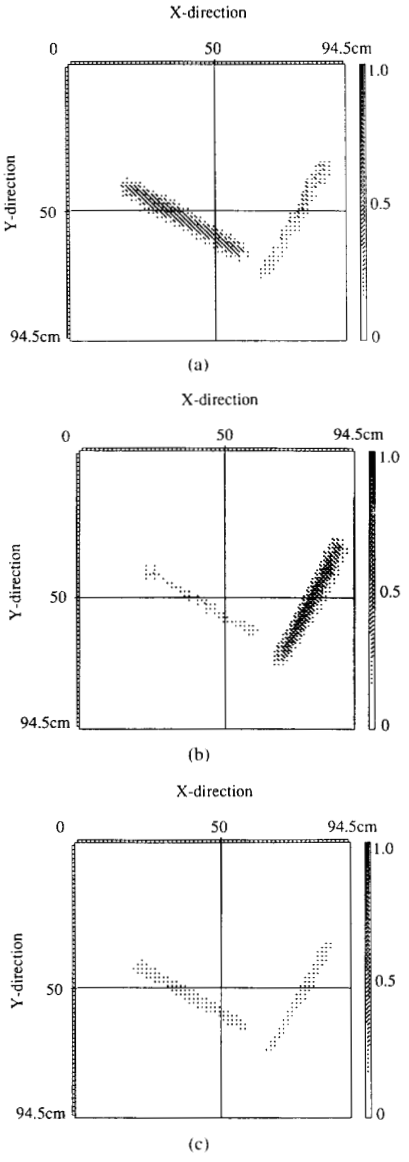

Fig. 6. Target images in the (HV) polarization basis:(a) HH, (b) VV, (c) HV.

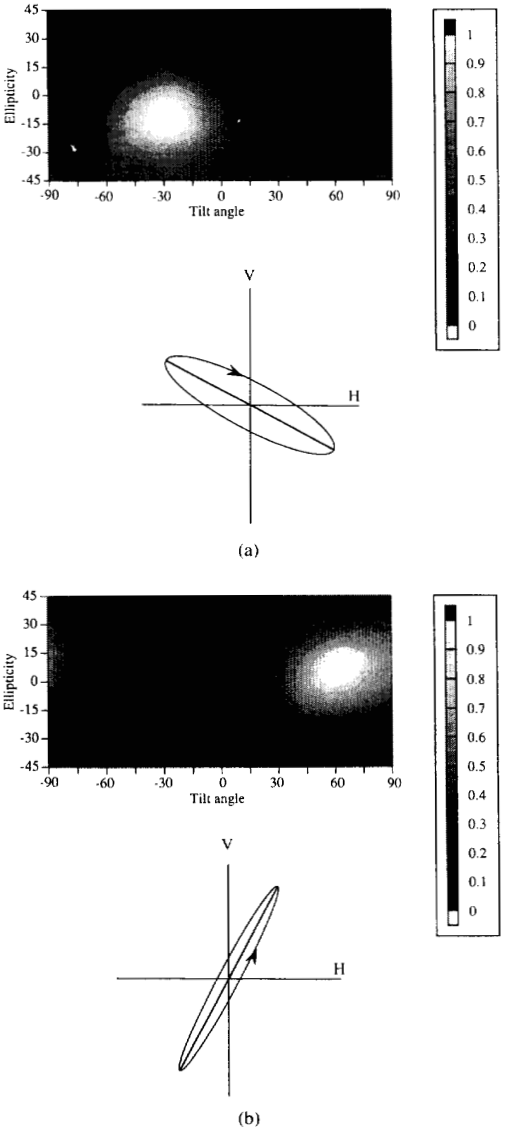

Fig. 7. Polarization signature and Co-Pol max polarization state:(a) target 1, (b) target 2.

We will implement (16) in a 2-D polarimetric imaging experiment which follows.

IV. 2-Dimensional Polarimetric Imaging

To confirm the applicability of this methodology, a 2-D imaging experiment was carried out in our laboratory. The target is a metallic pipe of 0.6 cmϕ × 50 cm that can be regarded as a linear target. Two pipes were placed orthogonal to each other on an imaging (x-y) plane as shown in Fig. 4. Fig. 4 shows a planar view of the 2-D measurement. The angle between the x-direction and target 1 is $-30°$, while the angle for target 2 is 60°. The distance from the antennas and the imaging plane is 70 cm. The block diagram of the FM-CW radar is shown in Fig. 5. In this configuration, both transmitting and receiving antennas are separated (i.e., slightly bistatic), which allows one to carry out polarimetric measurement. The antennas are standard rectangular horns of precisely the same type operative within 8.2–9.2 GHz. the aperture size is 15 cm × 11 cm. The polarization combination is a set of H-H, H-V, and V-V, where H stands for polarization direction being parallel to the x-direction, and V to the y-direction, respectively. The number of sampling points both in the x- and y-directions is 64 × 64 with incremental width of 1.5 cm. The radar specifications are listed in Table I. The isolation level between Co-Pol channel and X-Pol channel was found to be less than -30 dB which is acceptable for this demonstration. The phase error due to this slightly bistatic measurement arrangement was calibrated by an extrapolation method as described in [11].

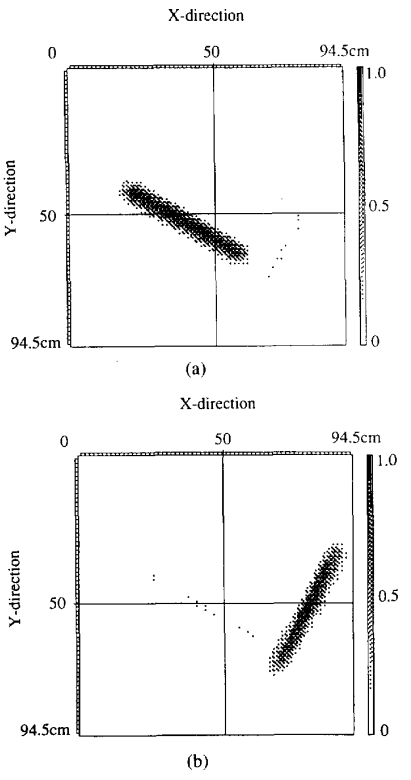

Fig. 8. Co-Pol maximum images: (a) target 1, (b) target 2.

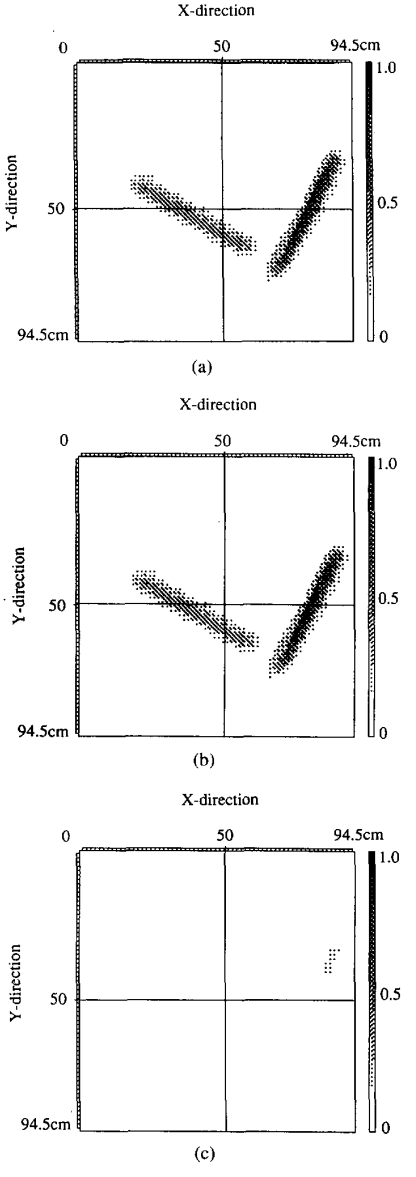

Fig. 9. Other polarimetric images: (a) Span image in the (*HV*) basis, (b) Span image in the (*AB*) basis, (c) X-Pol image in the (*AB*) basis.

A. *Imaging by Power*

The polarimetric measurement in the conventional (HV) basis produced 2-D images as shown in Fig. 6. These images are obtained from synthetic aperture processing at the radar range of $z = 70$ cm. It is seen that the target 1 appears strong in the HH image [Fig. 6(a)], whereas target 2 appears strong in the VV image [Fig. 6(b)], and that both targets are of the same magnitude in the HV image [Fig. 6(c)].

From the processing results of Fig. 6, it is possible to extract target reflection coefficients (complex amplitude, i.e., magnitude and phase) in each pixel. Therefore each pixel should have a scattering matrix with four elements assuming that $S_{HV} \approx S_{HV}$ although the slightly bistatic measurement adopted in the experiment. Now, we choose pixel values of target 1 and target 2 at the center position of their images in Fig. 6, which are expressed correspondingly by the scattering matrices

target 1:

$$[S_1] = \begin{bmatrix} -0.7656 - j0.0902 & 0.3529 - j0.1807 \\ 0.3529 - j0.1807 & -0.2056 + j0.2405 \end{bmatrix},$$

target 2:

$$[S_2] = \begin{bmatrix} -0.0640 + j0.4191 & -0.2378 + j0.2607 \\ -0.2378 + j0.2607 & -0.0961 + j0.8162 \end{bmatrix}.$$

Using the optimization procedure for the scattering matrices of targets 1 and 2, it is possible to determine the optimal characteristic polarization states. The polarization ratios of the Co-Pol maximum (=X-Pol null) are found to be

$$\rho_1 = 1.822 + j0.435 \quad \text{for target 1, and}$$
$$\rho_2 = -0.498 - j0.294 \quad \text{for target 2,}$$

which correspond to the characteristic polarization states of $\tau = -28.2°$, $\varepsilon = -13.1°$ for target 1, and $\tau = 62.3°$, $\varepsilon = 5.6°$ for target 2, respectively. The polarization ellipses together with these polarimetric signatures are illustrated in Fig. 7, where we can see that the corresponding tilt angles of the ellipse are very close to the actual target orientations. Since these targets are orthogonally placed, the Co-Pol max polarization states are expected to be orthogonal to one another.

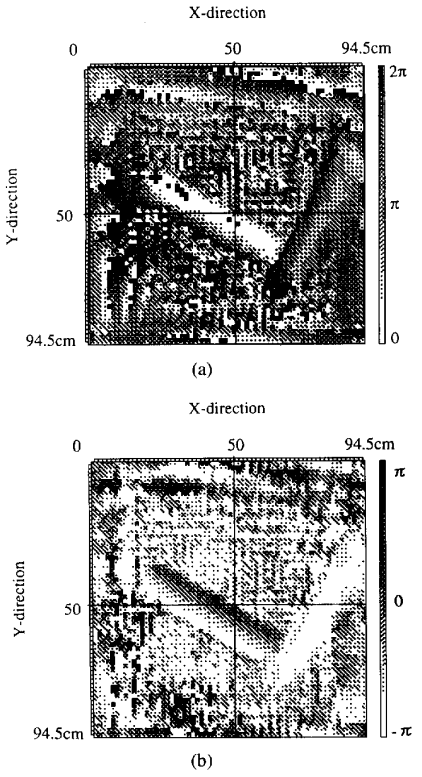

Fig. 10. Phase images in the (AB) polarization basis: (a) ϕ_{AB}, (b) $\frac{1}{2}1(\phi_{AA} - \phi_{BB})$.

This can also be checked by the orthogonality relation

$$\rho_1\rho_2^* = -1.0352 + j0.319 \approx -1.$$

Although the above relation is not strictly satisfied due to measurement errors and because of monostatic approximation is used, the results show that the polarimetric FM-CW imaging radar theory applies to the polarimetric target reflection coefficients.

Fig. 8 shows the Co-Pol maximum images for both targets 1 and 2, respectively. The polarization ratio ρ_1, and the resultant state of $[1, \rho_1]^T$ or equivalently $(\tau = -28.2°, \varepsilon = -13.1°)$ are used to calculate all pixels in the 2-D scene, enhancing the target 1 while suppressing target 2 in Fig. 8(a). It can be seen that target 2 is almost suppressed by the characteristic polarization state of target 1 because the orientation of the target 2 is orthogonal to target 1. Conversely, the same is true for the image in Fig. 8(b), where the polarization state is matched to target 2. This result shows that the polarimetric theory is applicable to the 2-D FM-CW imaging radar principle.

Next, the span images and the X-Pol image in the (AB) basis are illustrated in Fig. 9. The polarization basis (AB) means a basis such that "A" is the polarization state of $[1, \rho_1]^T$ that maximizes target 1 and "B" is orthogonal to "A". Since, the span image is independent of polarization basis, the same image is obtained in both the (HV) basis and the (AB) basis. On the other hand, the X-Pol (i.e., AB) image does not show any anticipated image, because the power is small enough to depict the scene. It is understood from Figs. 8–9 that any polarimetric contrast enhancement imaging is possible by implementation of the 2-D FM-CW radar data.

B. Imaging by Phase

If the scattering matrices in a 2-D scene are given, it is possible to depict images based on phase of the scattering matrix element. If the amplitude of the scattering matrix is small or contaminated by noise due to small target reflection amplitudes, phase imaging may be preferable for target mapping because the phase range is limited within 0 to 2π. Two phase images based on ϕ_{AB} and $\frac{1}{2}(\phi_{AA} - \phi_{BB})$ of the previous 2-D scene in the (AB) polarization basis are illustrated in Fig. 10, where the phase term ϕ_{AB} is defined such that

$$\phi_{AB} = \arg(S_{AB}), \quad 0 < \phi_{AB} < 2\pi.$$

The phase term $\frac{1}{2}(\phi_{AA} - \phi_{BB})$ is related to target principal curvatures [12], and is expected to play a dominant role in high resolution polarimetric imaging [13].

The target locations can be recognized in both phase images of Fig. 10. The ϕ_{AB} image provides two target locations which cannot be obtained by the corresponding power image of Fig. 9(c). The $\frac{1}{2}(\phi_{AA} - \phi_{BB})$ image are close to the ϕ_{AB} image, however, the interpretation in detail needs to be investigated in the future because the phase is derived from a wideband signal of FM-CW radar.

V. Conclusion

In this paper, the principle of radar polarimetry was applied to the 2-D synthetic aperture FM-CW radar imaging. Since the beat spectrum obtained by the radar has a complex amplitude bearing target information, we regarded it as an element of the scattering matrix to incorporate the polarimetric theory in FM-CW imaging. The validity of the replacement in the 2-D case was confirmed by a polarimetric imaging experiment in our laboratory, where two orthogonally placed metallic pipes were employed. Although there exist some measurement errors inherent with the FM-CW radar system, it was shown that 2-D polarimetric imaging was possible. Also polarimetric phase imaging using the scattering matrix was carried out to show the usefulness of target mapping when the corresponding amplitudes of the scattering matrix were very small. This polarimetric phase imaging may be useful for target detection in a lossy medium such as snow, sand, or soil, and this subject will be treated in the near future.

References

[1] J. A. Kong Ed., *PIER3 Progress in Electromagnetics Research: Polarimetric Remote Sensing*. New York: Elsevier, 1990.
[2] W.-M. Boerner *et al.*, *Direct and Inverse Methods in Radar Polarimetry*, parts 1 and 2, NATO ASI Series C: Mathematical and Physical Sciences, vol. 350. New York: Kluwer, 1992.
[3] H. Mott, *Antennas for Radar and Communications—A Polarimetric Approach*. New York: Wiley, 1992.
[4] P. Dubois and J. J. van Zyl, "Polarization filtering of SAR data," *SPIE*, vol. 1748, *Radar Polarimetry*, pp. 309–320, 1992.

[5] W.-M. Boerner, M. Walther, and A. C. Segal. "The concept of the polarimetric matched signal & imaging filters: application to radar target versus speckle reduction & optimal background clutter discrimination in microwave sensing and imaging," *J. Advances Remote Sensing*, vol. 2, no. 1, pp. 219–252, Jan. 1993.
[6] W.-M. Boerner, W. L. Yan, A. Q. Xi, and Y. Yamaguchi, "On the basic principles of radar polarimetry: the target characteristic polarization state theory of Kennaugh, Huynen's polarization fork concept and its extension to the partially polarized case," *Proc. IEEE*, vol. 79, pp. 1538–1550, Oct. 1991.
[7] J. P. Fitch, *Synthetic Aperture Radar*. New York: Springer-Verlag, 1988.
[8] D. R. Wehner, *High Resolution Radar*. Norwood, MA: Artech House, 1987.
[9] Y. Yamaguchi, M. Mitsumoto, M. Sengoku, and T. Abe, "Synthetic aperture FM-CW radar applied to the detection of objects buried in snowpack," *IEEE Trans. Geosci. Remote Sensing*, vol. 32, pp. 11–18, Jan. 1994.
[10] Y. Yamaguchi and M. Sengoku, "Detection of objects buried in sandy ground by a synthetic aperture FM-CW radar," *IEICE Trans. Commun.*, vol. E76-B, no. 10, pp. 1297–1304, 1993.
[11] Y. Yamaguchi, T. Nishikawa, M. Sengoku, W.-M. Boerner, and H. J. Eom, "Fundamental study on synthetic aperture FM-CW radar polarimetry," *IEICE Trans. Commun.*, vol. E77-B, no. 1, Jan. 1994.
[12] B.-Y. Foo, S. K. Chaudhuri, and W.-M Boerner, "Polarization correction and extension of Kennaugh-Cosgriff target-ramp response equation to the bistatic case and applications to electromagnetic inverse scattering," *IEEE Trans. Antenna Propagat.*, vol. 38, pp. 964–972, July 1990.
[13] W.-M. Boerner, B.-Y. Foo, and H. J. Eom, "Interpretation of the relative polarimetric co-polarization phase term $(\phi_{HH} - \phi_{VV})$ in high resolution SAR imaging using the JPL CV-990 polarimetric L-band SAR image data sets," *IEEE Trans. Geosci. Remote Sensing*, vol. GRS–25, pp. 77–82, Jan. 1987.
[14] D. L. Mensa, *High Resolution Radar Cross-Section Imaging*. Norwood, MA: Artech House, 1991.

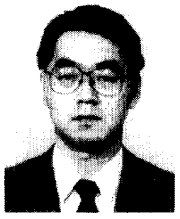

Yoshio Yamaguchi (M'83–SM'94) was born March 12, 1954, in Niigata, Japan. He received the B.E. degree in electronics engineering from Niigata University and the M.E. and Dr. Eng. degrees from Tokyo Institute Technology, Tokyo, Japan, in 1976, 1978, and 1983, respectively.

In 1978, he joined the Faculty of Engineering, Niigata University, where he is now an Associate Professor. From 1988 to 1989, he was a Research Associate at the University of Illinois, Chicago. His research interests are in the field of propagation characteristics of electromagnetic waves in lossy medium, radar polarimetry, microwave remote sensing and imaging.

Dr. Yamaguchi is a member of IEICE of Japan and the Japan Society for Snow Engineering.

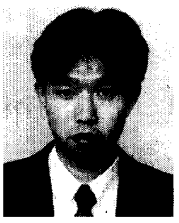

Toru Nishikawa was born April 25, 1969. He received the B.E. degree in information engineering from Niigata University, Niigata, Japan, in 1992.

He is engaged in polarimetric radar imaging.

Mr. Nishikawa is an associate member of the IEICE of Japan.

Masakazu Sengoku (S'70–M'72–SM'94) was born October 18, 1944, in Nagano Prefecture, Japan. He received the B.E. degree in electrical engineering from Niigata University, Niigata, Japan, and the M.E. and Ph.D. degrees from Hokkaido University, in 1967, 1969, and 1972, respectively.

In 1972, he joined the staff at Hokkaido University as a Research Associate. In 1978, he was an Associate Professor at Niigata University, where he is currently a Professor. During 1986–1987, he was a Visiting Scholar at the University of California, Berkeley, and at the University of Illinois, Chicago. His research interests include transmission of information, network theory, and graph theory.

Dr. Sengoku is a member of the IEICE of Japan and Japan Society for Industrial and Applied Mathematics. He is a recipient of the best paper award of the IEICE in 1992.

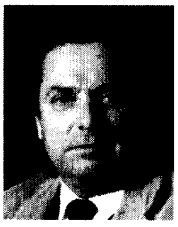

Wolfgang-Martin Boerner (S'66–M'67–SM'75–F'84) was born July 26, 1937, in Finschhafen, Papua-New Guinea. He received the B.S. degree from the Ausust von Platen Gymnasium, Ansbach, Germany, the M.Sc. degree from the Technical University of Munich, Munich, Germany, and the Ph.D. degree from the Moore School of Electrical Engineering, University of Pennsylvania, Philadelphia, in 1958, 1963, and 1967, respectively.

From 1967 to 1968, he was employed as a Research Assistant Engineer at the Department of Electrical and Computer Engineering, Radiation Laboratory, University of Michigan, Ann Arbor. From 1968 to 1978, he was with the Electrical Engineering Department, University of Manitoba, Winnipeg, Canada. In 1978, he joined the Department of Electrical Engineering and Computer Science, University of Illinois, Chicago, where he is a Professor of Electrical Engineering and Computer Science, and Director of the Communications and Sensing Laboratory.

Dr. Boerner is a recipient of the Alexander von Humboldt U.S. Senior Scientist Award and of the University of Illinois Senior Scholar Award. He served two terms as the Associate Editor of the IEEE TRANSACTIONS ON ANTENNAS AND PROPAGATION and as coeditor of the Journal on Inverse Methods.